Priming of microglia with IFN-γ slows neuronal gamma oscillations in situ

Thuy-Truc Ta[a], Hasan Onur Dikmen[a], Simone Schilling[a], Bruno Chausse[a], Andrea Lewen[a], Jan-Oliver Hollnagel[a], and Oliver Kann[a,b,1]

[a]Institute of Physiology and Pathophysiology, University of Heidelberg, D-69120 Heidelberg, Germany; and [b]Interdisciplinary Center for Neurosciences, University of Heidelberg, D-69120 Heidelberg, Germany

Edited by Lawrence Steinman, Stanford University School of Medicine, Stanford, CA, and approved January 23, 2019 (received for review August 6, 2018)

Type II IFN (IFN-γ) is a proinflammatory T lymphocyte cytokine that serves in priming of microglia—resident CNS macrophages—during the complex microglial activation process under pathological conditions. Priming generally permits an exaggerated microglial response to a secondary inflammatory stimulus. The impact of primed microglia on physiological neuronal function in intact cortical tissue (in situ) is widely unknown, however. We explored the effects of chronic IFN-γ exposure on microglia in hippocampal slice cultures, i.e., postnatal parenchyma lacking leukocyte infiltration (adaptive immunity). We focused on fast neuronal network waves in the gamma-band (30–70 Hz). Such gamma oscillations are fundamental to higher brain functions, such as perception, attention, and memory, and are exquisitely sensitive to metabolic and oxidative stress. IFN-γ induced substantial morphological changes and cell population expansion in microglia as well as moderate up-regulation of activation markers, MHC-II, CD86, IL-6, and inducible nitric oxide synthase (iNOS), but not TNF-α. Cytoarchitecture and morphology of pyramidal neurons and parvalbumin-positive inhibitory interneurons were well-preserved. Notably, gamma oscillations showed a specific decline in frequency of up to 8 Hz, which was not mimicked by IFN-α or IL-17 exposure. The rhythm disturbance was caused by moderate microglial nitric oxide (NO) release demonstrated by pharmacological microglia depletion and iNOS inhibition. In conclusion, IFN-γ priming induces substantial proliferation and moderate activation of microglia that is capable of slowing neural information processing. This mechanism might contribute to cognitive impairment in chronic brain disease featuring elevated IFN-γ levels, blood–brain barrier leakage, and/or T cell infiltration, well before neurodegeneration occurs.

interferon-gamma | microglia | neuroinflammation | neuronal electrical activity | nitric oxide synthase

Microglia are the resident CNS macrophages that become activated in most brain disorders, such as stroke, bacterial meningoencephalitis, multiple sclerosis, and Alzheimer's disease (1, 2). Activation of microglia is complex and features changes in morphology, antigen presentation, and cytokine and free radical release as well as migration and phagocytosis; its consequences range from neuroprotective to neurotoxic (3–7). However, the impact of different activated phenotypes on neuronal function is widely unknown (8–10).

Type II IFN (IFN-γ) is a soluble cytokine that is predominantly released from T helper type 1 (Th1) cells, cytotoxic T lymphocytes, and natural killer cells (4, 11). Notably, T cell infiltration and/or elevated IFN-γ have been reported in several neurologic disorders and animal models, including stroke, multiple sclerosis, and Alzheimer's disease (12–17). IFN-γ serves in the priming of microglia that associates with a variety of cellular adaptations, including changes in morphology, up-regulation of receptors, and increased levels of proinflammatory cytokines (4, 18–20). Notably, priming has been generally considered to permit an exaggerated microglial response to secondary—and otherwise subthreshold—inflammatory stimuli (20–24). For example, bacterial lipopolysaccharide (LPS) acting through Toll-like receptor 4 (TLR4) then triggers the release of proinflammatory and cytotoxic substances, such as TNF-α, IL-6, and nitric oxide (NO), finally resulting in neuronal death (1, 3, 25, 26). However, the impact of IFN-γ–primed microglia on synaptic activity and neural information processing has been widely unexplored (9, 23).

We addressed this fundamental question in postnatal brain tissue (in situ), i.e., organotypic hippocampal slice cultures (7, 10). Slice cultures feature well-preserved cytoarchitecture and functional neuronal networks, whereas they inherently lack leukocyte infiltration from blood vessels during experimental exposures (27–30). Cholinergic gamma oscillations (30–70 Hz) were used as a sensitive functional readout of precise synaptic transmission between excitatory pyramidal neurons and inhibitory interneurons (31, 32).

Results

Microglial Priming and Slowing of Gamma Oscillations. We exposed slice cultures (Fig. 1*A*) to recombinant IFN-γ at different concentrations for 72 h ("chronic") in the presence of a serum component to explore its full priming potential in microglia (5, 25). IFN-γ induced prominent changes in the morphology of microglia (Fig. 1*B*). Specifically, there was a more homogeneous Iba1 staining pattern, microglial hypertrophy with gradual reduction of ramification associated with shortening and flattening of cellular processes as well as pronounced spatial overlap of

Significance

Priming with classic lymphocyte cytokine, interferon-gamma (IFN-γ) is crucial during the complex activation process of tissue macrophages, such as microglia in the CNS, under pathological conditions. According to current biological concepts, priming permits an exaggerated macrophage immune response given a secondary inflammatory stimulus like bacterial components occurs. Here, we demonstrate that priming with IFN-γ itself induces proliferation and moderate activation of microglia, including up-regulation of inducible nitric oxide synthase (iNOS). Importantly, the concomitant moderate release of nitric oxide (NO) is sufficient to disturb fast neuronal network oscillations (30–70 Hz) that underlie higher brain functions, such as perception, attention, and memory. This mechanism might contribute to early cognitive impairment in chronic brain disorders, such as multiple sclerosis and Alzheimer's disease.

Author contributions: O.K. designed research; T.-T.T., H.O.D., S.S., B.C., and A.L. performed research; J.-O.H. contributed new reagents/analytic tools; T.-T.T., H.O.D., S.S., B.C., A.L., and J.-O.H. analyzed data; and O.K. wrote the paper.

The authors declare no conflict of interest.

This article is a PNAS Direct Submission.

[1]To whom correspondence should be addressed. Email: oliver.kann@physiologie.uni-heidelberg.de.

This article contains supporting information online at www.pnas.org/lookup/suppl/doi:10.1073/pnas.1813562116/-/DCSupplemental.

Published online February 19, 2019.

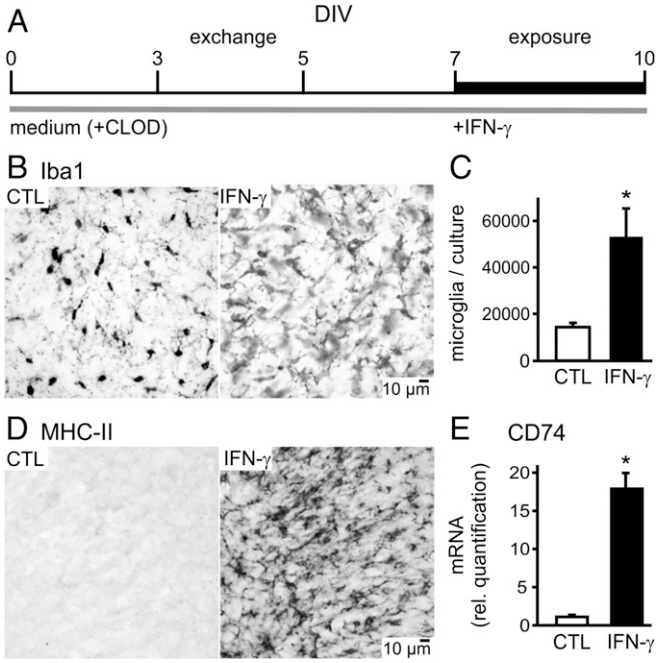

Fig. 1. Microglial morphology, cell numbers and markers. (*A*) Maintenance and exposure (+IFN-γ, 72 h) of rat hippocampal slice cultures in medium or medium plus clodronate (+CLOD) was done in the incubator. After 10 d in vitro (DIV), slice cultures and supernatant were analyzed with various methods. (*B*) Immunohistochemistry with the general marker Iba1 in naive control (CTL) and slice cultures exposed to IFN-γ (1,000 ng/mL). (*C*) Stereology-based cell counting of Iba1-positive cells. For *n*/*N* slices/preparations: CTL, 9/5; IFN-γ, 9/3. *$P < 0.001$, Mann-Whitney rank sum test. (*D*) Immunohistochemistry with the activation marker MHC-II in CTL and IFN-γ (1,000 ng/mL). (*E*) mRNA levels of CD74 (part of the MHC-II complex) were determined in tissue homogenates pooled from five slices, each. For *N* preparations: CTL, 4; IFN-γ (100 ng/mL, 24 h), 4; *$P < 0.001$ vs. CTL, unpaired *t* test. Sample images are taken from CA3 (Fig. 3).

microglia. Similar morphological changes have been reported in vitro and in vivo (18, 33, 34). The size of the microglial population increased 3.8-fold at the high concentration of IFN-γ (Fig. 1*C*). This substantial proliferation of microglia was associated with up-regulation of activation markers, such as MHC-II and CD86, and increased levels of IL-6; TNF-α was similar to naive control slice cultures (Figs. 1 *D* and *E* and 2*A* and *SI Appendix*, Fig. S1). The expression of inducible nitric oxide synthase (iNOS) (mRNA and protein level) and the concomitant release of nitric oxide (NO) were also increased (Fig. 2 *B*–*D*). These increases in IL-6, iNOS, and NO were moderate because the exposure of IFN-γ plus LPS, which served as a positive control, resulted in severalfold higher values (exaggerated microglial response, see below).

The cytoarchitecture of slice cultures as well as the morphology of excitatory pyramidal neurons and parvalbumin-positive inhibitory interneurons were well-preserved (Fig. 3 *A* and *B* and *SI Appendix*, Fig. S2). Notably, parvalbumin-positive inhibitory interneurons, such as fast-spiking GABAergic basket cells, contact the perisomatic region of excitatory pyramidal neurons and are essential for the emergence of cortical gamma oscillations in vivo and in situ (31, 35). Moreover, these interneurons are exquisitely sensitive to metabolic and oxidative stress (29, 32).

We next tested the functional integrity of the neuronal network by eliciting persistent gamma oscillations with acetylcholine (Fig. 3*C*) (29, 31). Gamma oscillations (30–70 Hz) were present in control and IFN-γ–exposed slice cultures (Fig. 4*A*). IFN-γ induced a clear decline in the frequency of gamma oscillations of up to 8 Hz, however (Fig. 4*B*). Peak power and full width at half-maximum (FWHM) were unchanged (Fig. 4 *C* and *D*). The latter oscillation properties primarily reflect number and synchronization of activated synapses. Albeit decreasing the frequency, IFN-γ did not affect the stability of gamma oscillations over time (Fig. 5). This rhythm slowing was specific because chronic exposures to IFN-α (type I IFN) or IL-17 (Th17 response) did not affect the properties of gamma oscillations (*SI Appendix*, Fig. S3) (36, 37).

Priming of microglia is supposed to result in an exaggerated microglial response to a secondary inflammatory stimulus (3, 20, 21). We tested this mechanism in situ using simultaneous (IFN-γ+LPS) and serial (IFN-γ→LPS) exposures to IFN-γ and LPS, at relatively low concentrations (3, 25). Notably, the single exposure to IFN-γ or LPS has either no or only minor effects on neuronal activity and survival in hippocampal slice cultures (Fig. 4 and *SI Appendix*, Fig. S4) (27, 38, 39). IFN-γ plus LPS induced strong iNOS expression and severalfold higher release of IL-6, TNF-α, and NO (Fig. 2*D* and *SI Appendix*, Fig. S2 *A*–*C*), similar to other reports (3, 5, 40). In addition, complete loss of neuronal activity and widespread inflammatory neurodegeneration occurred (*SI Appendix*, Fig. S2 *D* and *E*). This neurotoxic effect is mainly mediated by massive NO release (3, 39, 41). Thus, the

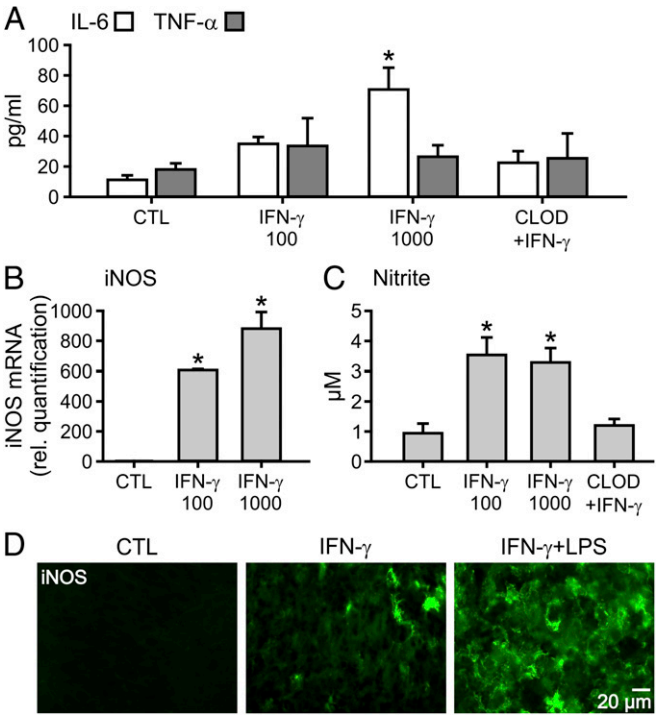

Fig. 2. Microglial cytokine release and iNOS expression. Slice cultures were exposed to IFN-γ or clodronate (100 μg/mL) plus IFN-γ (1,000 ng/mL) (CLOD+IFN-γ) for 72 h. (*A*) IL-6 and TNF-α levels in the culture medium. For *n*/*N* membranes/preparations: CTL, 4/4; IFN-γ (100 ng/mL), 4/4 (IL-6), and 5/4 (TNF-α); IFN-γ (1,000 ng/mL), 3/3 (IL-6), and 5/4 (TNF-α); CLOD+IFN-γ, 3/3 (IL-6), and 2/2 (TNF-α). *$P < 0.01$ vs. CTL and CLOD+IFN-γ, and < 0.05 vs. IFN-γ (100 ng/mL), one-way ANOVA with Tukey's post hoc test. (*B*) iNOS mRNA levels were determined in tissue homogenates pooled from five slices, each. For *N* preparations: CTL, 2; IFN-γ (100 ng/mL), 3; IFN-γ (1,000 ng/mL), 2. *$P < 0.01$ IFN-γ (100 ng/mL) and IFN-γ (1,000 ng/mL) vs. CTL, *$P < 0.05$ IFN-γ (1,000 ng/mL) vs. IFN-γ (100 ng/mL), one-way ANOVA with Tukey's post hoc test. (*C*) Nitrite levels reflecting NO release were determined in the culture medium. CTL, 5/5; IFN-γ (100 ng/mL), 6/5; IFN-γ (1,000 ng/mL), 6/5; CLOD+IFN-γ, 4/4. Each *$P < 0.05$ vs. CTL and CLOD+IFN-γ, one-way ANOVA with Tukey's post hoc test. (*D*) Immunohistochemistry of iNOS in CTL, IFN-γ (1,000 ng/mL), and IFN-γ (100 ng/mL) plus LPS (10 μg/mL) that served as a positive control. Sample images are taken from CA3 (Fig. 3).

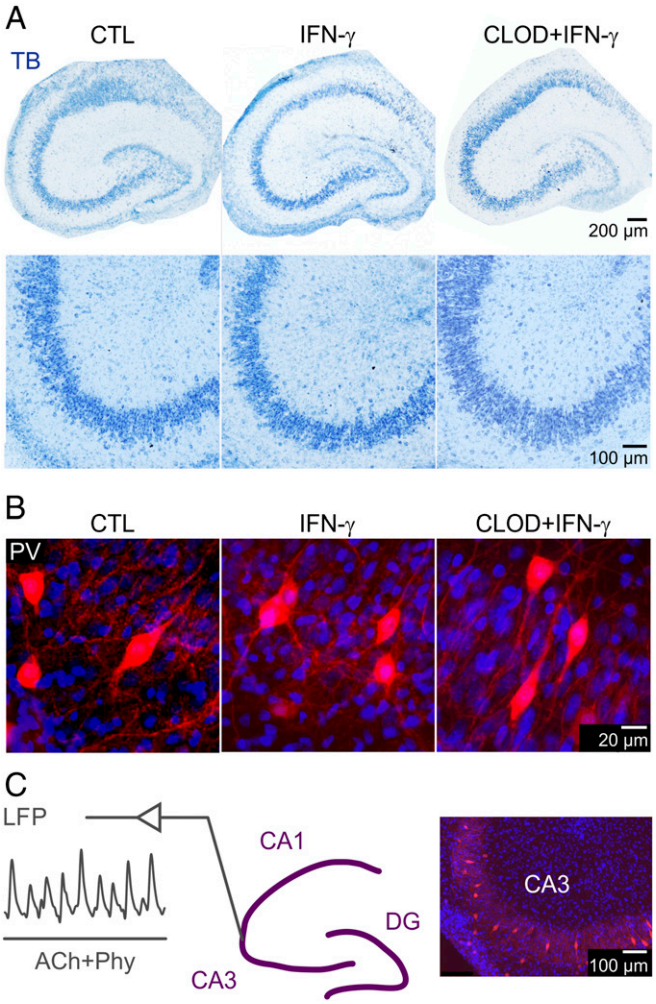

Fig. 3. Intact cytoarchitecture and neuronal morphology. Slice cultures were exposed to IFN-γ (1,000 ng/mL) or clodronate (100 µg/mL) plus IFN-γ (1,000 ng/mL) (CLOD+IFN-γ) for 72 h. (*A*) Toluidine blue (TB) staining. (*B*) Immunohistochemistry of parvalbumin-positive (PV) inhibitory interneurons. Sample images are taken from entire individual slice cultures (*A*, *Top*), the CA3 region (*A*, *Bottom*), and stratum pyramidale of CA3 (*B*). Note the well-preserved cytoarchitecture and neuronal morphology in all groups. (*C*) Gamma oscillations were elicited by acetylcholine (2 µM) and physostigmine (400 nM) (ACh+Phy, gray bar) at 34 ± 1 °C (*Left*). All local field potential (LFP) recordings were done in stratum pyramidale of CA3 (*Middle*); DG, dentate gyrus. Note the complex network of parvalbumin-positive interneurons that are essential for the emergence of gamma oscillations (*Right*).

exaggerated inflammatory response of primed microglia can be reliably replicated in slice cultures.

These foregoing findings suggest that priming of microglia with IFN-γ in situ is associated with moderate microglial activation and specific slowing of gamma oscillations.

Microglial iNOS-Mediated Slowing of Gamma Oscillations. IFN-γ receptors are functionally present in microglia, astrocytes, and, perhaps, in neurons (3, 42–44). To test whether slowing of gamma oscillations was mediated by microglia, we used liposome-encapsulated clodronate; this nontoxic bisphosphonate induces apoptosis specifically in macrophages/microglia after ingestion and intracellular accumulation (30, 39). Exposure to clodronate resulted in the almost complete depletion of microglia in otherwise untreated slice cultures (Fig. 6*A*). The residual microglial cells showed a more intense Iba1 staining and appeared more hypertrophic. IFN-γ was still capable of inducing proliferation of these microglia, even in the presence of clodronate. This might reflect the high self-renewal capacity of microglia (45). Notably, IFN-γ could not induce the specific decline in frequency in microglia-depleted slice cultures (CLOD+IFN-γ) (Fig. 6*A* and *SI Appendix*, Fig. S5). Peak power and FWHM were still unchanged. Possible side-effects of liposomes on gamma oscillations were excluded in control experiments (*SI Appendix*, Fig. S6). These data show that slowing gamma oscillations is primarily mediated by microglia rather than astrocytes in situ (41, 42).

We next tested whether the moderate microglial iNOS-mediated NO release was sufficient to disturb gamma oscillations. We used *N*-3-aminomethyl-benzyl-acetamidine (1400W) at low concentration (10 µM) (40, 41). The 1400W is a potent inhibitor of iNOS and selective over neuronal NOS (nNOS) and endothelial NOS (eNOS). Indeed, coapplication of 1400W (IFN-γ+1400W) prevented the slowing of gamma oscillations induced by IFN-γ (Fig. 6*B*). In addition, we observed an increase in peak power and a decrease in FWHM; these changes were also partially present in slice cultures exposed to 1400W alone. Conversely, acute application of the external NO-donor S-nitroso-*N*-acetyl-DL-penicillamine (SNAP) with the recording solution (positive control) decreased frequency and power of gamma oscillations in naive control cultures, whereas FWHM was unchanged (Fig. 6*C* and *SI Appendix*, Fig. S7). These effects occurred at a low SNAP concentration (100 µM) that is sufficient to elevate neuronal NO levels in slice cultures but far

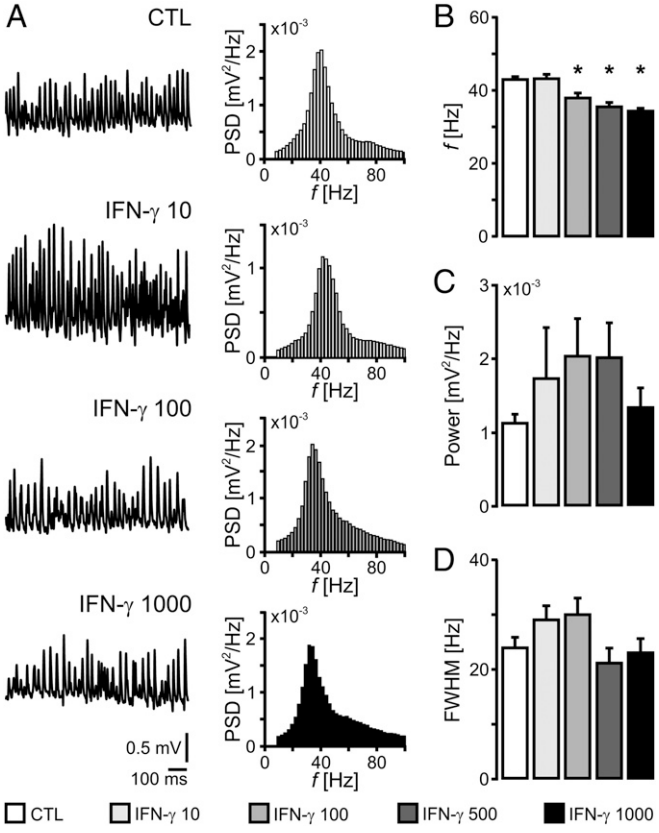

Fig. 4. Slowing of neuronal gamma oscillations. Slice cultures were exposed to different concentrations of IFN-γ for 72 h. (*A*) Sample traces of gamma oscillations (Fig. 3*C*) and corresponding power spectral density (PSD) calculated from data segments of 5 min. (*B*) Frequency (*f*), (*C*) power, and (*D*) FWHM were calculated from PSD in naive control (white) and exposed (black, gray shades) slice cultures. For *n*/*N* slices/preparations: CTL 25/5; IFN-γ (10 ng/mL), 13/3; IFN-γ (100 ng/mL), 17/3; IFN-γ (500 ng/mL), 13/3; IFN-γ (1,000 ng/mL), 18/4. Each $*P < 0.05$ vs. CTL, Kruskal-Wallis test with Dunn's post hoc test. Note the decline in frequency (*B*).

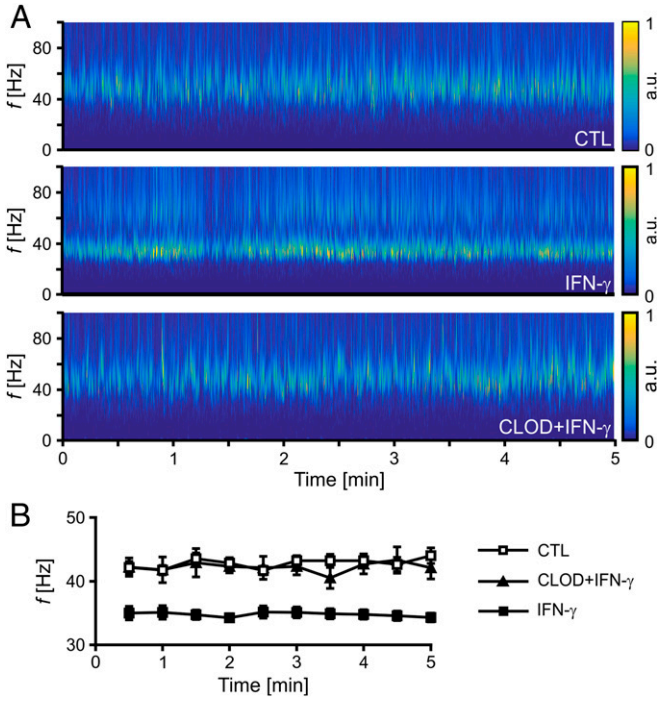

Fig. 5. Microglia-mediated slowing of gamma oscillations. Slice cultures were exposed to IFN-γ (1,000 ng/mL) and clodronate (100 μg/mL) plus IFN-γ (1,000 ng/mL) (CLOD+IFN-γ) for 72 h. (*A*) Sample spectrograms of gamma oscillations (Fig. 3*C*) were calculated from recordings in individual slices. Heat-scale colors encode for power in arbitrary units (a.u.). (*B*) Corresponding frequencies were calculated at 30-s intervals. For *n*/*N* slices/preparations: CTL, 25/5; IFN-γ, 18/4; CLOD+IFN-γ, 12/5. Note the stability of gamma oscillations over time in each group (two-way ANOVA with Holm-Sidak's post hoc test).

below the concentrations required to induce pathological seizure-like events (46). The additional effects of 1400W and SNAP on peak power and FWHM likely reflect complex interactions between nNOS-/iNOS-mediated NO release and the precise synaptic mechanisms underlying gamma oscillations (31, 47).

These foregoing complementary findings suggest that the specific slowing of gamma oscillations is primarily mediated by moderate iNOS up-regulation and concomitant NO release from microglia.

Discussion

Priming of Microglia with IFN-γ in Situ. IFN-γ is a dimerized soluble leukocyte cytokine and the only member of the type II IFN class. It is predominantly released from Th1 cells, cytotoxic T lymphocytes, and natural killer cells (4, 11). In many studies on microglial activation, IFN-γ has been traditionally used as a primer to evoke exaggerated microglial responses upon stimulation with microbial or endogenous ligands, such as bacterial LPS or amyloid-β peptide (3, 5, 26, 40). However, the effects of IFN-γ itself on microglial proliferation and activation, particularly in postnatal brain tissue (in situ), are less well-defined (8–10).

Slice cultures have been increasingly used to study the activation of microglia in situ, i.e., in the natural ("organotypic") environment with active neurons, astrocytes, and oligodendrocytes, and in the absence of leukocytes (7, 27, 28, 30). Under control conditions, slice cultures feature microglia with ramified morphology, low levels of activation markers, and minimal release of proinflammatory cytokines and NO (*SI Appendix*, *SI Discussion*). Notably, slice cultures exposed to different stimuli provide a reliable experimental model to explore the impact of different microglial phenotypes on the (dys)functions of individual neurons and neuronal networks (38, 39).

We exposed slice cultures to recombinant IFN-γ ranging from 10 to 1,000 ng/mL in the culture medium for 72 h. This experimental approach has been used in monocultures and microglia–neuron cultures (in vitro) to evoke maximal cytokine and NO release; within slice cultures, the final IFN-γ concentration might be lower because of prolonged diffusion distance, smaller extracellular space, and activity of proteinases, however (1, 3, 5, 25). We obtained a 1.9-fold (39) and a 3.8-fold microglial cell population expansion at 100 and 1,000 ng/mL IFN-γ, respectively, that went along with prominent morphological changes. Our data contrast with in vitro studies showing that IFN-γ had either no

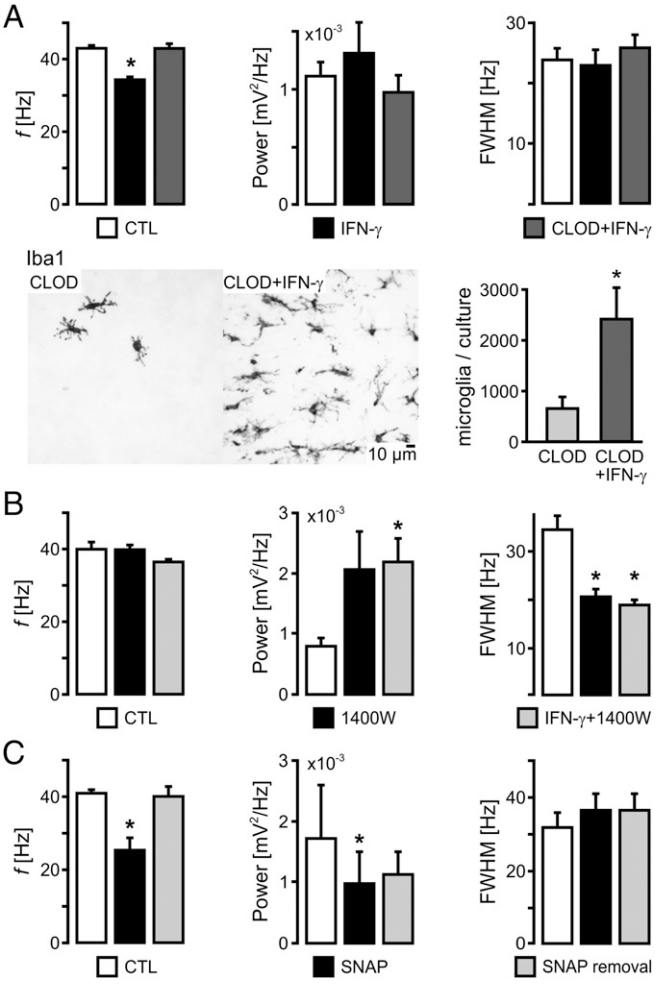

Fig. 6. Microglial iNOS-mediated slowing of gamma oscillations. Slice cultures were exposed to IFN-γ (1,000 ng/mL), clodronate (100 μg/mL) plus IFN-γ (1,000 ng/mL) (CLOD+IFN-γ), the iNOS inhibitor 1400W (10 μM), or IFN-γ plus 1400W (IFN-γ+1400W) for 72 h. Frequency (*f*), power, and FWHM of gamma oscillations (Fig. 3*C*) were calculated from power spectral density (PSD) in naive control (white) and exposed (black, gray shades) slice cultures. (*A, Top*) For *n*/*N* slices/preparations: CTL, 25/5; IFN-γ, 18/4; CLOD+IFN-γ, 12/5. **P* < 0.05 vs. CTL and CLOD+IFN-γ, Kruskal-Wallis test with Dunn's post hoc test. Note the absence of the decline in frequency in microglia-depleted slice cultures (CLOD+IFN-γ). (*A, Bottom*) Stereology-based cell counting of Iba1-positive cells. CLOD, 12/4; CLOD+IFN-γ, 17/4. **P* < 0.01, Mann-Whitney rank sum test. Note the magnitudes of microglial depletion (*Right*) and expansion (Fig. 1*C*). (*B*) CTL, 13/4; 1400W, 13/3; IFN-γ+1400W, 12/3. Each **P* < 0.05 vs. CTL, Kruskal-Wallis test with Dunn's post hoc test (*f*, power), one-way ANOVA with Holm-Sidak's post hoc test (FWHM). (*C*) Gamma oscillations in control condition, during acute application of SNAP (100 μM) and after SNAP removal. 17/7. Each **P* < 0.05 vs. CTL, Friedman test with Dunn's post hoc test (*f*, power), one-way repeated-measures ANOVA with Holm-Sidak's post hoc test (FWHM).

effect on microglial growth or even decreased microglial numbers (48, 49); this might reflect the use of mixed dissociated glial cell cultures from newborn rats and, perhaps, the absence of active neuronal networks. However, our in situ data basically replicate the effects of systemic and intracerebroventricular IFN-γ administration on microglial proliferation, including typical morphological changes in vivo (18, 20, 33). IFN-γ also moderately increased microglial activation markers, such as MHC-II, iNOS, and IL-6, but not TNF-α. This moderate microglial response likely reflects suppression by spontaneous neuronal activity (19, 29). We note that iNOS expression in astrocytes is negligible in slice cultures, even when exposed to IFN-γ and LPS (39, 40).

Similar features of primed microglia have been reported in the context of aging, traumatic CNS injury, and neurodegenerative disease in patients and animal models (15, 23, 34, 50). In view of these aspects, our data support the current concept of microglial priming (20, 23).

Slowing of Gamma Oscillations by Microglial NO Release in Situ. We tested the functional integrity of the local neuronal network in the hippocampal CA3 region, which is intrinsically capable of generating gamma oscillations (30–70 Hz) (29, 31). Gamma oscillations require precise chemical and electrical synaptic signaling between excitatory pyramidal neurons and inhibitory interneurons (31, 35). Among the latter, parvalbumin-positive, fast-spiking GABAergic basket cells featuring unique biophysical and bioenergetic properties have a key role in rhythm generation (31, 32). Gamma oscillations emerge in many cortical areas of the awake brain during sensory perception, selective attention, voluntary movement, and memory formation, and they feature high energy expenditure (29, 35, 51, 52). Therefore, gamma oscillations provide a sensitive functional readout of even discrete neuronal network dysfunction (32).

We found a decline in the frequency of gamma oscillations in slice cultures exposed to IFN-γ. This specific disturbance already occurred at 100 ng/mL IFN-γ; and it was absent in microglia-depleted slice cultures, widely excluding direct actions of IFN-γ on neurons (43). We recently showed that 100 ng/mL IFN-γ for 72 h increased the microglial cell number about 1.9-fold (39). Therefore, our findings suggest that the IFN-γ–mediated slowing of gamma oscillations requires, at least, the doubling of the local microglial population. Indeed, local microgliosis and astrogliosis are common characteristics of different brain disorders (1, 2, 7).

A few studies reported on chronic effects of IFN-γ on neuronal functions, such as hippocampal short-term and long-term synaptic plasticity, including cognitive performance (44, 53, 54). We show that IFN-γ also slows neuronal gamma oscillations that are fundamental to spike-timing–dependent plasticity and higher brain functions (31, 35). Importantly, we identify moderate iNOS up-regulation and concomitant NO release as the key factors that might cause neuronal dysfunctions. Our in situ data are widely in line with in vitro reports on IFN-γ–induced microglial NO release (3, 25, 55). Indeed, it is well-established that IFN-γ is one of the most typical inducers of iNOS in macrophages and microglia (1, 4, 11). The moderate NO release seems to be a specific response because IFN-γ widely failed to induce reactive oxygen species production in microglia, at least, in vitro (24, 56). Therefore, our data provide details for the current concept of microglial priming (20, 23), i.e., the presence of an inflammatory NO component that can disturb cortical gamma oscillations. We note that microglial priming with IFN-γ might differ from other priming scenarios, such as stress or prion disease models (21, 22).

NO has a complex physiological role in neurotransmission. NO release from constitutive nNOS is Ca^{2+}-dependent and occurs at certain pre- and postsynaptic sites of excitatory and inhibitory neurons (47). Thus, the increase of NO by up-regulation of microglial iNOS can even discretely disturb physiological neurotransmission associated with, for example, neuronal network oscillations and synaptic plasticity (57–59). Whether the related rhythm slowing reflects direct and/or synergistic NO-mediated alterations in the intrinsic biophysical properties of neurons, glutamatergic and $GABA_A$-receptor–mediated neurotransmission, and/or energy metabolism needs to be explored (*SI Appendix, SI Discussion*) (31, 32, 58, 60).

Slowing of gamma oscillations might significantly impair neural information processing in local cortical networks as well as information transfer between remote cortical networks, and well before neurodegeneration occurs (32, 35, 51, 52, 61). Such a general mechanism might apply to a variety of (chronic) clinical situations that are associated with elevated IFN-γ levels, blood–brain barrier leakage and/or T cell infiltration (*SI Appendix, SI Discussion*). Prominent examples are aging, (post) stroke, multiple sclerosis, and, perhaps, Alzheimer's disease (2, 9, 10, 23, 37, 62).

We provide in situ evidence that the priming step of microglia with IFN-γ features moderate microglial activation, including iNOS up-regulation that is capable of slowing neural information processing. Our study might contribute to the development of pharmacologic strategies for treating several neurologic and psychiatric disorders associated with low-grade inflammation.

Materials and Methods

More information is provided in *SI Appendix, SI Materials and Methods* and *SI Appendix, SI References*.

Slice Cultures and Exposures. Wistar rats (Charles River Laboratories) were handled in accordance with the European directive 2010/63/EU and with consent of the animal welfare officers at University of Heidelberg (licenses, T46/14 and T96/15). Hippocampal slice cultures were prepared from 9- to 10-d-old pups in sterile conditions and maintained on Biopore membranes at the interface between serum-containing culture medium (4 mM glucose) and humidified normal atmosphere enriched with 5% (vol/vol) CO_2 (36.5 °C) (29, 39). Cell culture materials were certified free of endotoxin and IFN-γ. Chemical depletion of microglia was achieved with liposome-encapsulated clodronate (Liposoma B.V.) (30, 39). Exposures to recombinant IFN-γ (PeproTech), 1400W (Sigma-Aldrich), and LPS (Enzo Life Sciences) were done in the dark.

Biochemical Analyses. Culture medium was sampled and rapidly frozen to –80 °C. Calibrations and biochemical analyses were performed in accordance with the manufacturer's instructions using a microplate reader (Bio-Rad Laboratories) (39). Samples were analyzed with ELISA kits (R&D Systems). NO release was derived from the concentration of its oxidation product, nitrite, with a Griess reaction-based assay (Merck Chemicals).

RNA Isolation and qRT-PCR. RNA isolation and cDNA synthesis were performed with the RNeasy Plus Mini kit (Qiagen) and High Capacity cDNA Reverse Transcription kit (Applied Biosystems), respectively. qPCR was carried out on a StepOnePlus Real-Time PCR System (Applied Biosystems) using TaqMan assays [MHC-II (CD74), iNOS, ACTB]. Gene expression was determined by comparative gene expression analysis; β-actin served as endogenous control.

Immunohistochemistry and Stereological Cell Counting. Slice cultures were fixed in 4% (vol/vol) paraformaldehyde and cut into thin (25 or 30 μm) sections with a cryostat (CM1850; Leica Microsystems). Microglia were stained with anti-Iba1 (WAKO Chemicals), anti-CD86 (Abcam), and anti-MHC-II (Abcam), neurons with toluidine blue (Sigma-Aldrich) and anti-parvalbumin (Sigma-Aldrich), and iNOS with anti-iNOS (Merck Chemicals). Primary antibodies were visualized with fluorescent or biotin-conjugated secondary antibodies. Stereological analyses were performed with Stereo Investigator (MBF Bioscience). Volume-corrected microglial cell counting was done using an optical fractionator probe (39).

Local Field Potential Recordings. After exposures, slice cultures were rapidly transferred to the recording chamber [95% (vol/vol) O_2, 5% (vol/vol) CO_2; 34 ± 1 °C] (29, 39). The recording solution contained 129 mM NaCl, 3 mM KCl, 1.25 mM NaH_2PO_4, 1.8 mM $MgSO_4$, 1.6 mM $CaCl_2$, 21 mM $NaHCO_3$, and 10 mM glucose (pH 7.3). The local field potential was recorded with microelectrodes connected to an amplifier (EXT 10–2F; npi electronic), low-pass–filtered at 3 kHz, and digitized at 10 kHz using CED 1401 interface and Spike2 software (Cambridge Electronic Design). Gamma oscillations were elicited by application of acetylcholine and physostigmine. Standard salts

and acetylcholine were purchased from Sigma-Aldrich, physostigmine was purchased from Tocris, and SNAP was purchased from Biomol.

Calculations and Statistics. Offline signal analysis of gamma oscillations was performed in MatLab 11.0 (The MathWorks). Data segments of 5 min were low-pass–filtered with a digital Butterworth algorithm at 200-Hz corner frequency and processed with Welch´s algorithm with a Hamming window size of 4,096 points for calculation of the power spectral density (bin size = 2.441 Hz). Spectrograms were derived from continuous wavelet transforms of a given recording using Morlet wavelets. Data are reported as mean ± SEM from slice cultures ("slices") (*n*) and independent preparations (*N*), unless stated otherwise. Statistical significance was determined in GraphPad Prism 6.0 (GraphPad Software); data distribution was tested with Shapiro-Wilk test. Statistical tests are specified in the legends.

ACKNOWLEDGMENTS. We thank Ismini E. Papageorgiou, Tiziana Cesetti, and Elke Pralle for valuable technical advice; Hilmar Bading and Otto Bräunling for technical support; and Amit Agarwal for critical discussion.

1. Colonna M, Butovsky O (2017) Microglia function in the central nervous system during health and neurodegeneration. *Annu Rev Immunol* 35:441–468.
2. Prinz M, Priller J (2017) The role of peripheral immune cells in the CNS in steady state and disease. *Nat Neurosci* 20:136–144.
3. Chao CC, Hu S, Molitor TW, Shaskan EG, Peterson PK (1992) Activated microglia mediate neuronal cell injury via a nitric oxide mechanism. *J Immunol* 149:2736–2741.
4. Colton CA (2009) Heterogeneity of microglial activation in the innate immune response in the brain. *J Neuroimmune Pharmacol* 4:399–418.
5. Häusler KG, et al. (2002) Interferon-γ differentially modulates the release of cytokines and chemokines in lipopolysaccharide- and pneumococcal cell wall-stimulated mouse microglia and macrophages. *Eur J Neurosci* 16:2113–2122.
6. Mazaheri F, et al. (2017) TREM2 deficiency impairs chemotaxis and microglial responses to neuronal injury. *EMBO Rep* 18:1186–1198.
7. Ransohoff RM, Perry VH (2009) Microglial physiology: Unique stimuli, specialized responses. *Annu Rev Immunol* 27:119–145.
8. Hanisch U-K, Kettenmann H (2007) Microglia: Active sensor and versatile effector cells in the normal and pathologic brain. *Nat Neurosci* 10:1387–1394.
9. Klein RS, Garber C, Howard N (2017) Infectious immunity in the central nervous system and brain function. *Nat Immunol* 18:132–141.
10. Ransohoff RM (2016) How neuroinflammation contributes to neurodegeneration. *Science* 353:777–783.
11. Mosser DM, Edwards JP (2008) Exploring the full spectrum of macrophage activation. *Nat Rev Immunol* 8:958–969.
12. Browne TC, et al. (2013) IFN-γ production by amyloid β-specific Th1 cells promotes microglial activation and increases plaque burden in a mouse model of Alzheimer's disease. *J Immunol* 190:2241–2251.
13. Giunti D, et al. (2003) Phenotypic and functional analysis of T cells homing into the CSF of subjects with inflammatory diseases of the CNS. *J Leukoc Biol* 73:584–590.
14. Heesen C, et al. (2006) Fatigue in multiple sclerosis: An example of cytokine mediated sickness behaviour? *J Neurol Neurosurg Psychiatry* 77:34–39.
15. Murphy ÁC, Lalor SJ, Lynch MA, Mills KHG (2010) Infiltration of Th1 and Th17 cells and activation of microglia in the CNS during the course of experimental autoimmune encephalomyelitis. *Brain Behav Immun* 24:641–651.
16. Togo T, et al. (2002) Occurrence of T cells in the brain of Alzheimer's disease and other neurological diseases. *J Neuroimmunol* 124:83–92.
17. Yilmaz G, Arumugam TV, Stokes KY, Granger DN (2006) Role of T lymphocytes and interferon-γ in ischemic stroke. *Circulation* 113:2105–2112.
18. Grau V, Herbst B, van der Meide PH, Steiniger B (1997) Activation of microglial and endothelial cells in the rat brain after treatment with interferon-gamma in vivo. *Glia* 19:181–189.
19. Neumann H, Boucraut J, Hahnel C, Misgeld T, Wekerle H (1996) Neuronal control of MHC class II inducibility in rat astrocytes and microglia. *Eur J Neurosci* 8:2582–2590.
20. Perry VH, Holmes C (2014) Microglial priming in neurodegenerative disease. *Nat Rev Neurol* 10:217–224.
21. Cunningham C, Wilcockson DC, Campion S, Lunnon K, Perry VH (2005) Central and systemic endotoxin challenges exacerbate the local inflammatory response and increase neuronal death during chronic neurodegeneration. *J Neurosci* 25:9275–9284.
22. Frank MG, Baratta MV, Sprunger DB, Watkins LR, Maier SF (2007) Microglia serve as a neuroimmune substrate for stress-induced potentiation of CNS pro-inflammatory cytokine responses. *Brain Behav Immun* 21:47–59.
23. Norden DM, Muccigrosso MM, Godbout JP (2015) Microglial priming and enhanced reactivity to secondary insult in aging, and traumatic CNS injury, and neurodegenerative disease. *Neuropharmacology* 96:29–41.
24. Spencer NG, Schilling T, Miralles F, Eder C (2016) Mechanisms underlying interferon-γ-induced priming of microglial reactive oxygen species production. *PLoS One* 11: e0162497.
25. Dawson VL, Brahmbhatt HP, Mong JA, Dawson TM (1994) Expression of inducible nitric oxide synthase causes delayed neurotoxicity in primary mixed neuronal-glial cortical cultures. *Neuropharmacology* 33:1425–1430.
26. Meda L, et al. (1995) Activation of microglial cells by β-amyloid protein and interferon-γ. *Nature* 374:647–650.
27. Ajmone-Cat MA, Mancini M, De Simone R, Cilli P, Minghetti L (2013) Microglial polarization and plasticity: Evidence from organotypic hippocampal slice cultures. *Glia* 61:1698–1711.
28. Daria A, et al. (2017) Young microglia restore amyloid plaque clearance of aged microglia. *EMBO J* 36:583–603.
29. Kann O, Huchzermeyer C, Kovács R, Wirtz S, Schuelke M (2011) Gamma oscillations in the hippocampus require high complex I gene expression and strong functional performance of mitochondria. *Brain* 134:345–358.
30. Vinet J, et al. (2012) Neuroprotective function for ramified microglia in hippocampal excitotoxicity. *J Neuroinflammation* 9:27.
31. Hájos N, Paulsen O (2009) Network mechanisms of gamma oscillations in the CA3 region of the hippocampus. *Neural Netw* 22:1113–1119.
32. Kann O (2016) The interneuron energy hypothesis: Implications for brain disease. *Neurobiol Dis* 90:75–85.
33. Kong G-Y, Kristensson K, Bentivoglio M (2002) Reaction of mouse brain oligodendrocytes and their precursors, astrocytes and microglia, to proinflammatory mediators circulating in the cerebrospinal fluid. *Glia* 37:191–205.
34. Monsonego A, et al. (2006) Abeta-induced meningoencephalitis is IFN-γ-dependent and is associated with T cell-dependent clearance of Abeta in a mouse model of Alzheimer's disease. *Proc Natl Acad Sci USA* 103:5048–5053.
35. Buzsáki G, Wang X-J (2012) Mechanisms of gamma oscillations. *Annu Rev Neurosci* 35: 203–225.
36. Li W, et al. (2018) Microglia have a more extensive and divergent response to interferon-α compared with astrocytes. *Glia* 66:2058–2078.
37. McManus RM, Mills KHG, Lynch MA (2015) T cells-protective or pathogenic in Alzheimer's disease? *J Neuroimmune Pharmacol* 10:547–560.
38. Hellstrom IC, Danik M, Luheshi GN, Williams S (2005) Chronic LPS exposure produces changes in intrinsic membrane properties and a sustained IL-β-dependent increase in GABAergic inhibition in hippocampal CA1 pyramidal neurons. *Hippocampus* 15:656–664.
39. Papageorgiou IE, et al. (2016) TLR4-activated microglia require IFN-γ to induce severe neuronal dysfunction and death in situ. *Proc Natl Acad Sci USA* 113:212–217.
40. Duport S, Garthwaite J (2005) Pathological consequences of inducible nitric oxide synthase expression in hippocampal slice cultures. *Neuroscience* 135:1155–1166.
41. Bal-Price A, Brown GC (2001) Inflammatory neurodegeneration mediated by nitric oxide from activated glia-inhibiting neuronal respiration, causing glutamate release and excitotoxicity. *J Neurosci* 21:6480–6491.
42. Carpentier PA, et al. (2005) Differential activation of astrocytes by innate and adaptive immune stimuli. *Glia* 49:360–374.
43. Mizuno T, et al. (2008) Interferon-γ directly induces neurotoxicity through a neuron specific, calcium-permeable complex of IFN-γ receptor and AMPA GluR1 receptor. *FASEB J* 22:1797–1806.
44. Monteiro S, et al. (2016) Absence of IFNγ promotes hippocampal plasticity and enhances cognitive performance. *Transl Psychiatry* 6:e707.
45. Tay TL, et al. (2017) A new fate mapping system reveals context-dependent random or clonal expansion of microglia. *Nat Neurosci* 20:793–803.
46. Kovács R, et al. (2009) Endogenous nitric oxide is a key promoting factor for initiation of seizure-like events in hippocampal and entorhinal cortex slices. *J Neurosci* 29:8565–8577.
47. Hardingham N, Dachtler J, Fox K (2013) The role of nitric oxide in pre-synaptic plasticity and homeostasis. *Front Cell Neurosci* 7:190.
48. Giulian D, Ingeman JE (1988) Colony-stimulating factors as promoters of ameboid microglia. *J Neurosci* 8:4707–4717.
49. Kloss CUA, Kreutzberg GW, Raivich G (1997) Proliferation of ramified microglia on an astrocyte monolayer: Characterization of stimulatory and inhibitory cytokines. *J Neurosci Res* 49:248–254.
50. Sierra A, Gottfried-Blackmore AC, McEwen BS, Bulloch K (2007) Microglia derived from aging mice exhibit an altered inflammatory profile. *Glia* 55:412–424.
51. Melloni L, et al. (2007) Synchronization of neural activity across cortical areas correlates with conscious perception. *J Neurosci* 27:2858–2865.
52. van Vugt MK, Schulze-Bonhage A, Litt B, Brandt A, Kahana MJ (2010) Hippocampal gamma oscillations increase with memory load. *J Neurosci* 30:2694–2699.
53. Maher FO, Clarke RM, Kelly A, Nally RE, Lynch MA (2006) Interaction between interferon γ and insulin-like growth factor-1 in hippocampus impacts on the ability of rats to sustain long-term potentiation. *J Neurochem* 96:1560–1571.
54. Vikman KS, Owe-Larsson B, Brask J, Kristensson KS, Hill RH (2001) Interferon-γ-induced changes in synaptic activity and AMPA receptor clustering in hippocampal cultures. *Brain Res* 896:18–29.
55. Goodwin JL, Uemura E, Cunnick JE (1995) Microglial release of nitric oxide by the synergistic action of β-amyloid and IFN-γ. *Brain Res* 692:207–214.
56. Colton CA, Yao J, Keri JE, Gilbert D (1992) Regulation of microglial function by interferons. *J Neuroimmunol* 40:89–98.
57. Fuentealba P, et al. (2008) Ivy cells: A population of nitric-oxide-producing, slow-spiking GABAergic neurons and their involvement in hippocampal network activity. *Neuron* 57:917–929.
58. Neitz A, et al. (2014) Postsynaptic NO/cGMP increases NMDA receptor currents via hyperpolarization-activated cyclic nucleotide-gated channels in the hippocampus. *Cereb Cortex* 24:1923–1936.
59. Selvakumar B, et al. (2013) S-nitrosylation of AMPA receptor GluA1 regulates phosphorylation, single-channel conductance, and endocytosis. *Proc Natl Acad Sci USA* 110:1077–1082.
60. Chen Z, et al. (2014) Microglial displacement of inhibitory synapses provides neuroprotection in the adult brain. *Nat Commun* 5:4486.
61. Mably AJ, Colgin LL (2018) Gamma oscillations in cognitive disorders. *Curr Opin Neurobiol* 52:182–187.
62. Montagne A, et al. (2015) Blood-brain barrier breakdown in the aging human hippocampus. *Neuron* 85:296–302.